

Supplementary information

Scavenging of superoxide by a membrane bound superoxide oxidase

Camilla A.K. Lundgren,^{1†} Dan Sjöstrand,^{1†*} Olivier Biner,^{2†} Matthew Bennett,¹ Axel Rudling,³ Ann-Louise Johansson,¹ Peter Brzezinski,¹ Jens Carlsson,³ Christoph von Ballmoos^{2*} and Martin Högbom^{1*}

Affiliations:

¹ Department of Biochemistry and Biophysics, Stockholm University, 10691 Stockholm, Sweden.

² Department of Chemistry and Biochemistry, University of Bern, Bern, Switzerland.

³ Science for Life Laboratory, Department of Cell and Molecular Biology, Uppsala University, Uppsala, Sweden.

† Contributed equally

* Correspondence to: hogbom@dbb.su.se (M.H.), christoph.vonballmoos@dcb.unibe.ch (C.vB.), dan.sjostrand@dbb.su.se (D.S.)

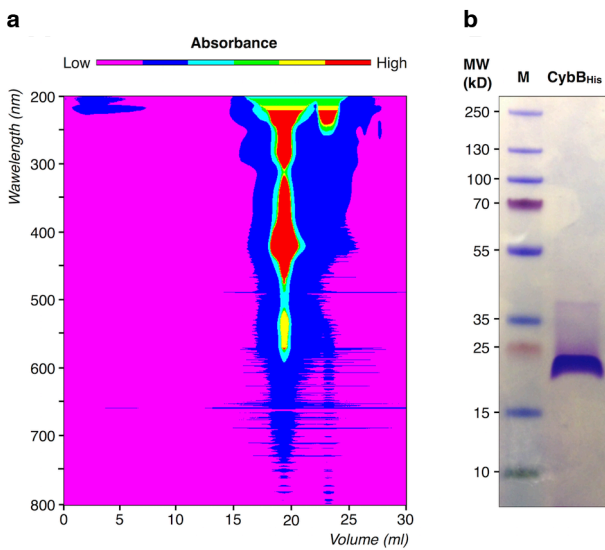
Supplementary Table 1: Measured rate constants for reaction with superoxide.

	$k_{\text{measured}} [\text{M}^{-1}\text{s}^{-1}]$	$k_{\text{published}} [\text{M}^{-1}\text{s}^{-1}]$
SOD		2×10^9 (ref ⁴⁰)
cyt c	$(4.62 \pm 1.83) \times 10^5$	6×10^5 (ref ²⁷)
CybB (Prep. 1)	$(4.22 \pm 1.76) \times 10^7$	
CybB (Prep. 2)	$(1.12 \pm 0.28) \times 10^8$	

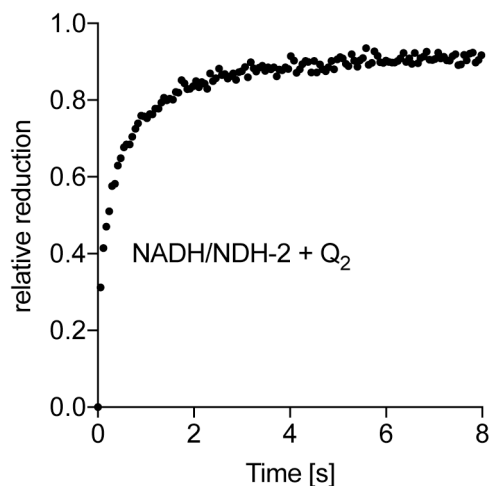
Supplementary Table 2. Crystallographic data and refinement statistics

	Refinement	Phasing
Data collection		
Space group	C 2 2 2 ₁	C 2 2 2 ₁
Cell dimensions		
a, b, c (Å)	68.05, 91.10, 97.92	68.37, 91.48, 98.32
α, β, γ (°)	90, 90, 90	90, 90, 90
	<i>Peak</i>	
Wavelength	0.97973	0.97973
Resolution (Å)	20.0–1.97 (2.09–1.97)	50.0–1.97 (2.09–1.97)
R_{meas}	10.3 (121.2)	8.4 (97.6)
$I / \sigma I$	14.38 (2.00)	13.67 (2.09)
Completeness (%)	99.7 (99.1)	99.9 (99.3)
Redundancy	13.0 (13.2)	7.0 (6.9)
Refinement		
Resolution (Å)	20.0–1.97	
No. reflections	20754 / 1093	
$R_{\text{work}} / R_{\text{free}}$	0.1876 / 0.2044	
No. atoms		
Protein	1414	
Ligand/ion	132	
Water	25	
<i>B</i> -factors		
Protein	52.7	
Ligand/ion	50.1	
Water	46.3	
R.m.s deviations		
Bond lengths (Å)	0.0178	
Bond angles (°)	1.8294	

*Values in parentheses are for highest-resolution shell.

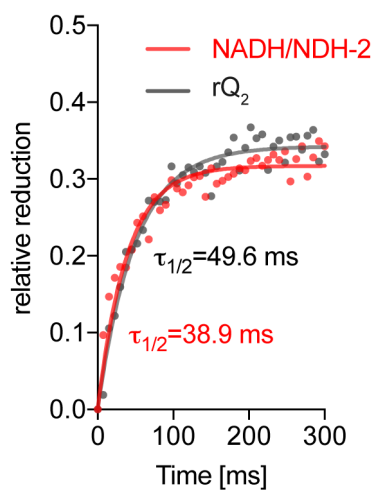


Supplementary Fig. 1. Purification of CybB. (a) Absorbance "heat map" (wavelength vs. time) from size exclusion chromatography of CybB with diode array detection. In addition to the standard protein UV range absorbance (i.e. tyrosine/tryptophan absorbance at 280 nm), the deep red CybB protein also absorbs in the visible light range, notably at the ~420 nm (Soret) and ~560 nm heme *b* absorbance peaks. (b) SDS-PAGE gel of purified CybB_{His}. The protein runs as a single band at its expected molecular weight (~21,8 kD). This experiment has been repeated more than 10 times with similar results.

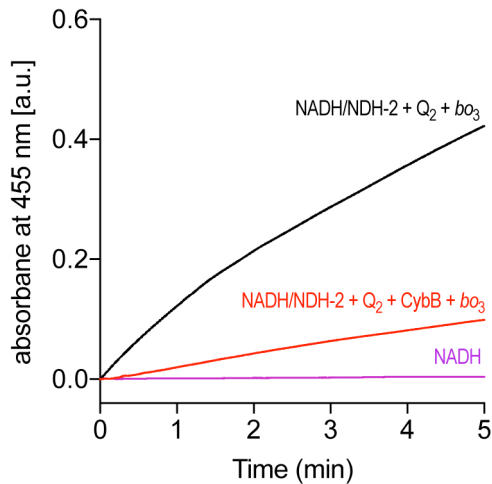


Supplementary Fig. 2. Reduction of CybB by a combination of NADH/NDH-2 and ubiquinone

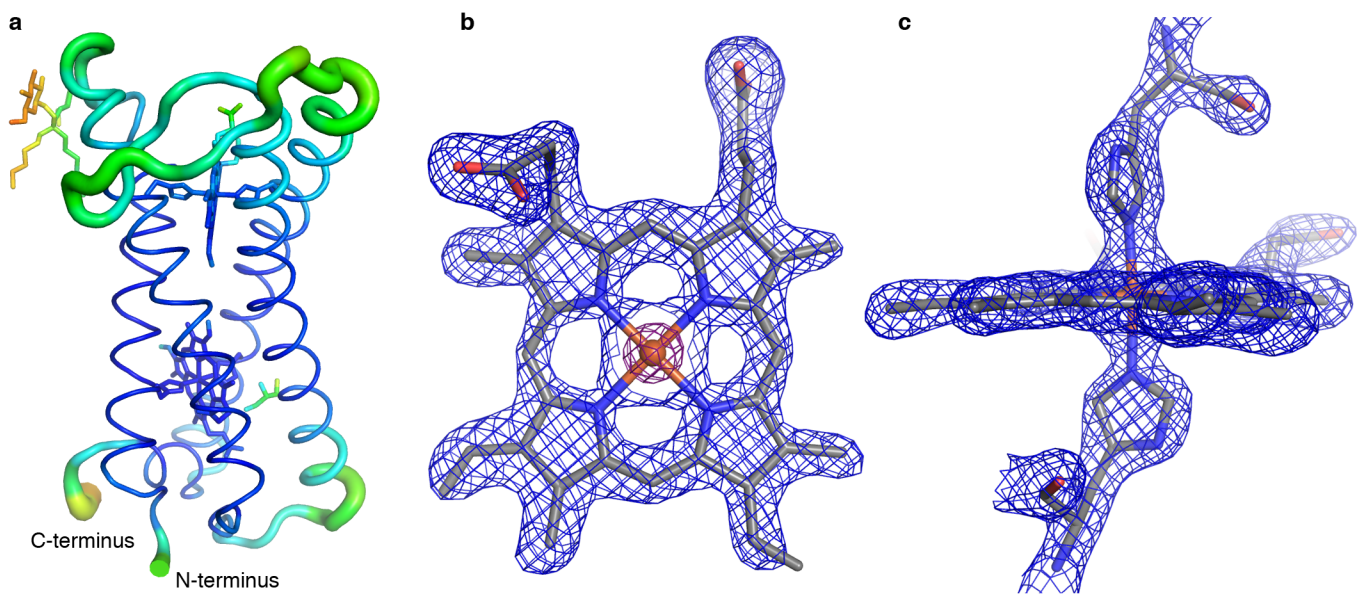
Q₂. NADH, NDH-2, and ubiquinone Q₂ were pre-incubated for 1 min leading to efficient production of both superoxide and reduction of ubiquinone Q₂. Mixing of the solution with detergent solubilized CybB rapidly and completely reduced the CybB (rate limited by mixing). The kinetic trace shown is a representative of at least 3 independent measurements.



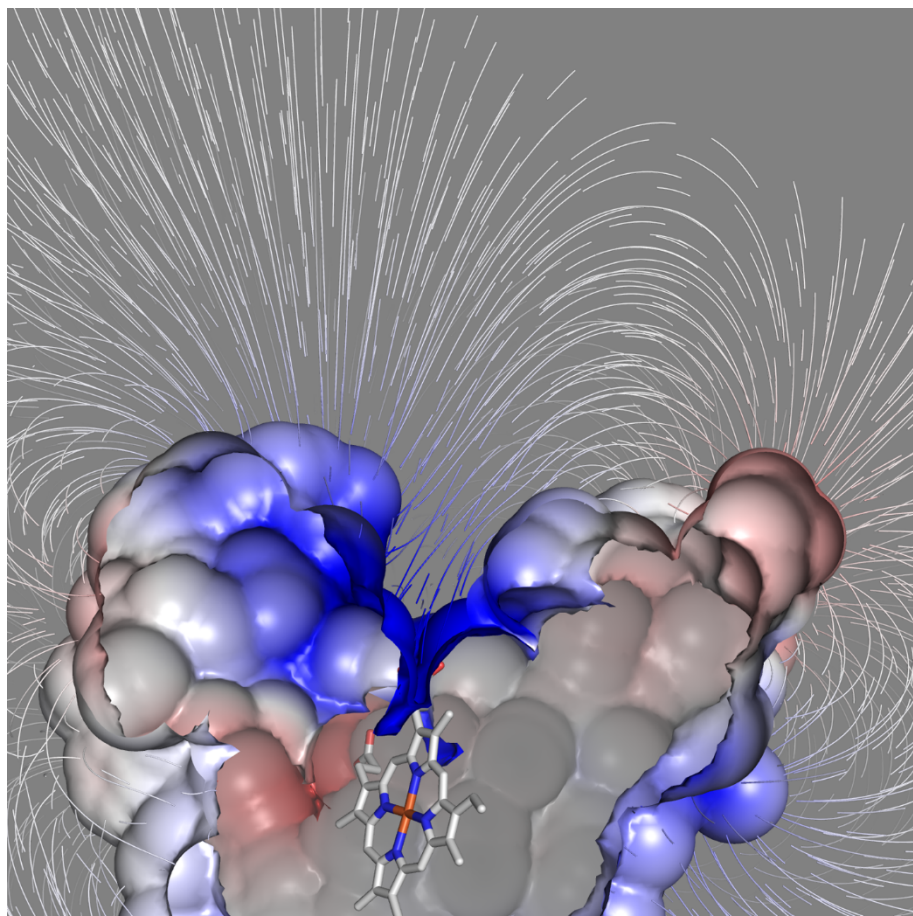
Supplementary Fig. 3. Stopped-flow kinetics of CybB reduction. Stopped-flow kinetic analysis showed that reduction of CybB with ubiquinol Q₂H₂ and NADH/NDH-2 is a fast and specific process with time constants of 40-50 ms. The kinetic trace shown is a representative of at least 3 independent measurements.



Supplementary Fig. 4. Superoxide-production assay with NADH/NDH-2. Superoxide-production was monitored by following the reduction of WST-1 at 455 nm. NADH/NDH-2 (black trace) together with ubiquinone Q₂ and bo₃ oxidase (black trace) leads to a linear production of superoxide, which is depleted by further addition of CybB (red trace). The kinetic trace shown is a representative of at least 3 independent measurements.

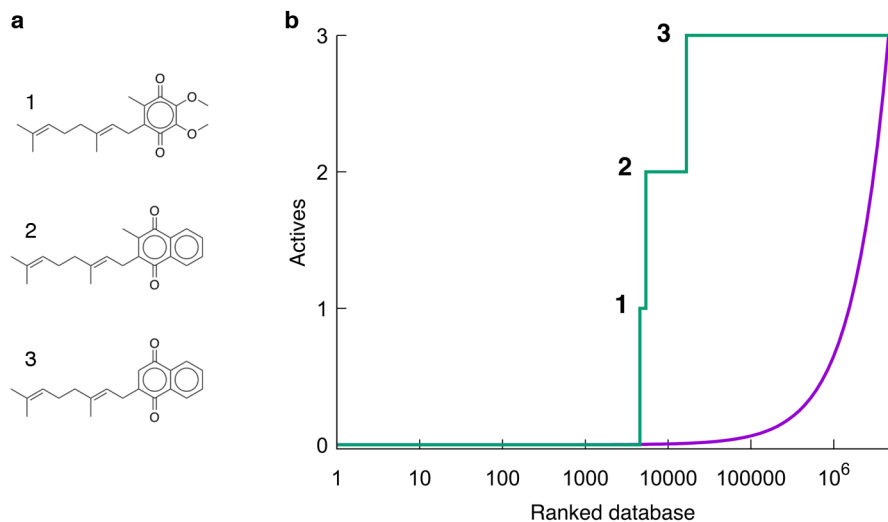


Supplementary Fig. 5. (a) Cartoon representation of protein structure B-factors. The highest B-factors are observed in the termini and the loop structures protruding from the membrane on the periplasmic side. The RSRZ score (14%) for the protein is worse than average for a structure at this resolution. The main reason for this is the dynamic loop structures on the periplasmic side comprising residues 106-136 where most of the residues with high RSR reside. (b and c) Electron density around hemes 1 and 2 respectively. 2Fo-Fc electron density map contoured at 2 σ (blue) and 10 σ (purple).

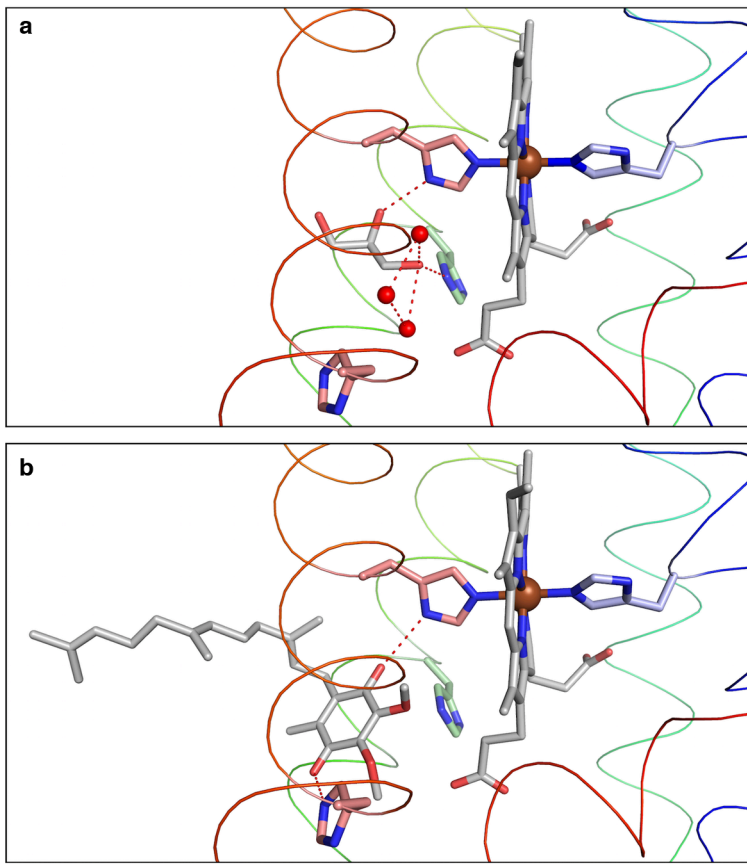


Supplementary Fig. 6. Electrostatic properties of the periplasmic surface of CybB.

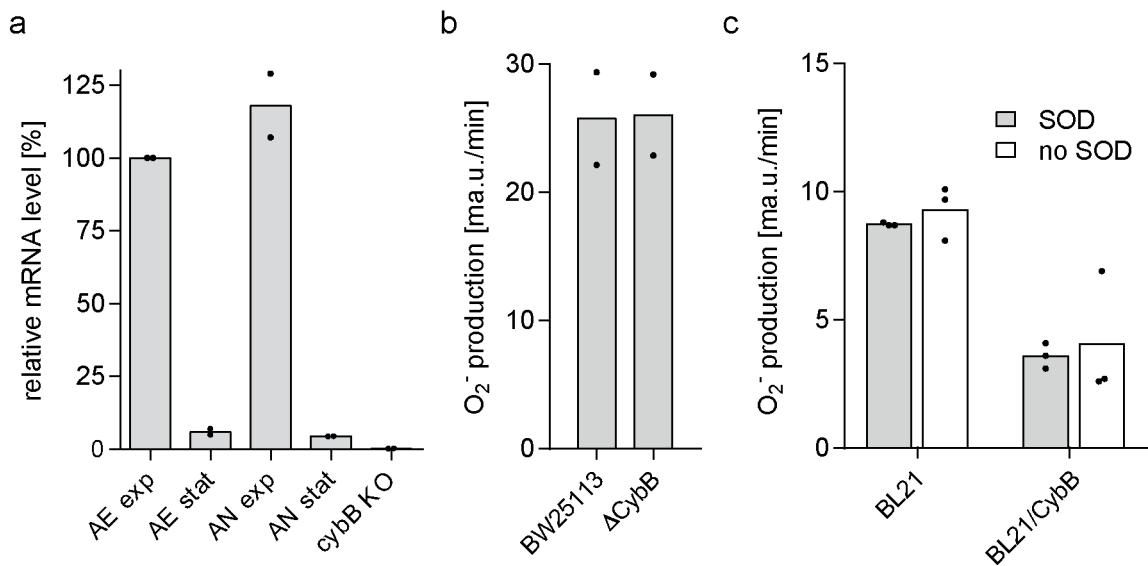
Electrostatic potential mapped onto the solvent accessible surface of CybB (blue positive, red negative). Electrostatic field lines are indicated. Electrostatics were calculated using APBS⁵⁴ including both hemes and displayed using the APBS plugin in PyMol.



Supplementary Fig. 7. Docking of quinone headgroups. (a) 2D structures of quinone headgroups representing ubiquinone (1), menaquinone (2), and demethylmenaquinone (3). (b) The three quinone headgroups were seeded into a database of 4.6 million commercially available compounds that was docked to the crystal structure. Enrichment of the quinones by the binding site was quantified using a receiver operator characteristic curve (ROC) based on the docking energy scores. The number of quinones (actives or true positives) identified (y-axis) versus the ranking of the compounds in the database (x-axis) is shown. A strong enrichment of quinones (green line) compared to random selection (purple line) was obtained.



Supplementary Fig. 8: Structure-docking model comparison. (a) The structure of the suggested quinone-binding cavity of CybB with bound glycerol. Three waters in the cavity coordinate the glycerol molecule (all other waters were removed for clarity). It should be noted that there is some residual unmodeled density in the proximity of the modeled glycerol suggesting that there may be a larger ligand with low occupancy or a mixture of ligands bound at this site. (b) *In silico* generated docking model of ubiquinone-3 binding to CybB. The position and binding mode of the docked ubiquinone shows striking resemblance to the glycerol from the crystal structure. Notably, the glycerol is in approximately the same position and orientation as the upper edge of the ubiquinone ring, with two oxygens from each molecule positioned almost identically, including the quinone carbonyl oxygen coordinated by the heme-binding histidine. Moreover, the glycerol-coordinating waters occupy a similar space in the pocket as the ubiquinone "arms" do in the docking model.



Supplementary Fig. 9. (a) Relative mRNA levels of *cybB* under different growth conditions.

Relative mRNA levels of *cybB*, normalized to the mRNA level of a housekeeping gene (*idnT*), was determined by RT-qPCR of *E. coli* BW25113 grown under aerobic (AE) and anaerobic (AN) conditions. Shown are *cybB* mRNA levels of samples taken during exponential (exp) and stationary phase (stat). As control, *cybB* transcript levels of a *cybB* knock-out strain (KO) was determined. Shown are the mean values and the individual data points from n=2 biologically independent experiments (each measured in technical replicates).

(b) Superoxide production from respiring *E. coli* wt and *cybB* knockout membranes.

Superoxide production from respiring *E. coli* membranes normalized to NADH consumption. Membrane vesicles from the *E. coli* control strain BW25113 expressing wild-type levels of CybB compared with membranes isolated from the *cybB*-knockout strain. Shown are the mean values and the individual data points from n=2 biologically independent experiments (each measured in technical triplicates). **(c) Superoxide production from respiring *E. coli* wt and CybB overexpressing membranes.** Membrane vesicles from *E. coli* strain BL21 pLysS expressing the wild-type CybB compared with membranes isolated from CybB-overexpressing cells. Addition of SOD to the vesicles did not affect the superoxide detection by WST-1 under aerobic conditions. Shown are the mean values and the individual data points from n=3 biologically independent experiments.

NP_415935 HIGHLVIVIYLFFIALPVIGLVMYNR--GNPWFAG-L-TMPYSEA-NFERRVDSLK---SWHETANLYGVIGLEHAAALAHYFWKNTTLLRMPKRK
 YP_403372 HIGHLVIVIYLFFIALPVIGLVMYNR--GNPWFAG-L-TMPYSEA-NFERRVDSLK---SWHETANLYGVIGLEHAAALAHYFWKNTTLLRMPKRK
 NP_460598 HIGHLVIVIYLFFIALPVIGLVMYNR--GNPWFAG-L-TMPYSEA-NFERRVDSLK---SWHETANLYGVIGLEHAAALAHYFWKNTTLLRMPKRK
 YP_003612579 HIGHLVIVIYLFFIALPVIGLVMYNR--GNPWFAG-L-TMPYSEA-NFERRVDSLK---SWHETANLYGVIGLEHAAALAHYFWKNTTLLRMPKRK
 YP_002348217 HVGHWVIVIYLFFIALPVIGLVMYNR--GNPWFAG-L-TMPYSEA-NFERRVDSLK---SWHETANLYGVIGLEHAAALAHYFWKNTTLLRMPKRK
 NP_416483 SLMIMLITFLAIPLLGIALMWAYS---GKSWSFLG-FNVSPPFVTP-SEKALIK---RHEMLANMSYFVIGHALAILHYVIKNTTLLRMPKRK
 NP_460220 KIMHILYIYLFFIALPVIGLVMYNR--GNPWFAG-L-TMPYSEA-NFERRVDSLK---SWHETANLYGVIGLEHAAALAHYFWKNTTLLRMPKRK
 WP_002211611 RISHWGLYIYLFFIALPVIGLVMYNR--GNPWFAG-L-TMPYSEA-NFERRVDSLK---SWHETANLYGVIGLEHAAALAHYFWKNTTLLRMPKRK
 NP_249609 RIMHYAUYLMMGIPFAGNLILSA--GKIPFFG-LELPPLVDK-NPDLAGQK---EWETIGNAGYFLIGHAAALAHYFWKNTTLLRMPKRK
 NP_246256 HSVOMLILCILITPIGFVFTLAD--ADDFMLG-MNLPS--LEISLG---KAHNSFIALGQHAAALAHYFWKNTTLLRMPKRK
 NP_416483 KAHNLVYIYLFFIALPVIGLVMYNR--GNPWFAG-L-TMPYSEA-NFERRVDSLK---SWHETANLYGVIGLEHAAALAHYFWKNTTLLRMPKRK
 NP_298617 NATHIMLYIYLFFIALPVIGLVMYNR--GNPWFAG-L-TMPYSEA-NFERRVDSLK---SWHETANLYGVIGLEHAAALAHYFWKNTTLLRMPKRK
 NP_252265 KAGHFLYIYLFFIALPVIGLVMYNR--GNPWFAG-L-TMPYSEA-NFERRVDSLK---SWHETANLYGVIGLEHAAALAHYFWKNTTLLRMPKRK
 NP_232647 KAGHGLLIAITAMPGLAG---KRPLDLFPLWLVQIGPFDFL--EAKVAFAG---GTRVTVQYLLFALLIGHAAALAHYFWKNTTLLRMPKRK
 NP_520840 EGHHVIVIYLFFIALPVIGLVMYNR--GNPWFAG-L-TMPYSEA-NFERRVDSLK---SWHETANLYGVIGLEHAAALAHYFWKNTTLLRMPKRK
 NP_105780 PLHHLAYAFOVALPISGNALVSVSTLEITMPFNLFVMPNPLTESDAESFWA---LAHWYLAIGLALVALVAARLHFLLRSVLTMRP
 NP_385543 RATHSLIYLFFIALPVIGLVMYNR--GNPWFAG-L-TMPYSEA-NFERRVDSLK---SWHETANLYGVIGLEHAAALAHYFWKNTTLLRMPKRK
 NP_354489 RUVHSALLITFLAVGAWAVSVSTLPAIPSYFLNLIIIPHLPLPKSGTSEAFWA---DVTIATYLAIVLVLVHAAALAHYFWKNTTLLRMPKRK
 NP_287191 KAGHAAVIVIYLFFIALPVIGLVMYNR--GNPWFAG-L-TMPYSEA-NFERRVDSLK---SWHETANLYGVIGLEHAAALAHYFWKNTTLLRMPKRK
 NP_460129 AAGHLLYIYLFFIALPVIGLVMYNR--GNPWFAG-L-TMPYSEA-NFERRVDSLK---SWHETANLYGVIGLEHAAALAHYFWKNTTLLRMPKRK
 NP_002211010 VTHMLMYSIECMISGYLISTAD--GPIINVGFAPVTLAG-LPDAOADAG---TLYLAIVLVLVHAAALAHYFWKNTTLLRMPKRK
 NP_249113 KIGHALYIYLFFIALPVIGLVMYNR--GNPWFAG-L-TMPYSEA-NFERRVDSLK---SWHETANLYGVIGLEHAAALAHYFWKNTTLLRMPKRK
 NP_232928 KSAHIMYIYLFFIALPVIGLVMYNR--GNPWFAG-L-TMPYSEA-NFERRVDSLK---SWHETANLYGVIGLEHAAALAHYFWKNTTLLRMPKRK
 NP_542051 ALGHGLYIYLFFIALPVIGLVMYNR--GNPWFAG-L-TMPYSEA-NFERRVDSLK---SWHETANLYGVIGLEHAAALAHYFWKNTTLLRMPKRK
 NP_542019 RULHGFLYIYLFFIALPVIGLVMYNR--GNPWFAG-L-TMPYSEA-NFERRVDSLK---SWHETANLYGVIGLEHAAALAHYFWKNTTLLRMPKRK
 NP_518320 RULHGFLYIYLFFIALPVIGLVMYNR--GNPWFAG-L-TMPYSEA-NFERRVDSLK---SWHETANLYGVIGLEHAAALAHYFWKNTTLLRMPKRK
 consensus 1.....10.....20.....30.....40.....50.....60.....70.....80.....90.....100.....110.....aa

Supplementary Fig. 10. Sequence alignment of diverse CybB homologues. Sequence alignment of a number of diverse representative sequences belonging to the COG3038 and PRK11513 groups of the Cytochrome_b_N Superfamily (NCBI accession number cl23723). Arrows indicate heme Fe-coordinating residues, red oval indicate residues potentially involved in proton transfer from the cytoplasm.

Sequences are denoted with their NCBI accession numbers. The top sequence represents *E. coli* SOO (NP_415935). The other sequences are homologous proteins from the following organisms: *Agrobacterium fabrum* NP_354489; *Brucella melitensis* NP_542019, NP_542051; *Enterobacter cloacae* YP_003612579; *Escherichia coli* NP_416483, NP_287191; *Mesorhizobium loti* NP_105468, NP_105780; *Pasteurella multocida* NP_246256; *Pseudomonas aeruginosa* NP_249113, NP_249609, NP_252265; *Ralstonia solanacearum* NP_518320, NP_520840; *Salmonella enterica* NP_460129, NP_460220, NP_460598; *Shigella dysenteriae* YP_403372; *Sinorhizobium meliloti* NP_385543; *Vibrio cholerae* NP_232647, NP_232928; *Xylella fastidiosa* NP_298617; *Yersinia pestis* YP_002348217, WP_002211010 WP_002211611. It should be noted that the eukaryotic B₅₆₁³⁷ belongs to different protein families (but also within the Cytochrome_b_N Superfamily).

Compared to SOO, the eukaryotic B₅₆₁ family has a different number of TM helices and opposite membrane insertion topology of the heme-coordinating helices. They also show no quinone binding site. Still, since they display strikingly analogous heme architecture and positively charged patch with an exposed heme edge, studies on their reactivity with superoxide would be interesting.